Journal of Intelligent & Robotic Systems (2020) 100:925–944
https://doi.org/10.1007/s10846-020-01253-6

Pose Selection and Feedback Methods in Tandem Combinations of Particle Filters with Scan-Matching for 2D Mobile Robot Localisation

Alexandros Filotheou[1] · Emmanouil Tsardoulias[1] · Antonis Dimitriou[1] · Andreas Symeonidis[1] · Loukas Petrou[1]

Received: 25 October 2019 / Accepted: 28 August 2020 / Published online: 15 September 2020

Abstract

Robot localisation is predominantly resolved via parametric or non-parametric probabilistic methods. The particle filter, the most common non-parametric approach, is a Monte Carlo Localisation (MCL) method that is extensively used in robot localisation, as it can represent arbitrary probabilistic distributions, in contrast to Kalman filters, which is the standard parametric representation. In particle filters, a weight is internally assigned to each particle, and this weight serves as an indicator of a particle's estimation certainty. Their output, the tracked object's pose estimate, is implicitly assumed to be the weighted average pose of all particles; however, we argue that disregarding low-weight particles from this averaging process may yield an increase in accuracy. Furthermore, we argue that scan-matching, treated as a prosthesis of (or, put differently, fit in tandem with) a particle filter, can also lead to better accuracy. Moreover, we study the effect of feeding back this improved estimate to MCL, and introduce a feedback method that outperforms current state-of-the-art feedback approaches in accuracy and robustness, while alleviating their drawbacks. In the process of formulating these hypotheses we construct a localisation pipeline that admits configurations that are a superset of state-of-the-art configurations of tandem combinations of particle filters with scan-matching. The above hypotheses are tested in two simulated environments and results support our argumentation.

Keywords Robot Localisation · Particle Filters · Scan-matching

1 Introduction

Mobile robot localisation is a well-studied field in robotics, and several diverse approaches to localisation have been proposed in the past. Probabilistic methods [1] have been applied to the task of localisation and proved their success and robustness to sensor noise, map discrepancies with regard to a robot's operating environment, motion model discrepancies with regard to the true kinematics of the robot, and pose uncertainty. As for sensors, laser range finders are popular devices employed in robot localisation due to their measurement accuracy, real-time operability, and virtually no need for preprocessing.

Particle filters [2] comprise a probabilistic method for tackling the robot localisation problem, arising from the need for a robot to be more flexible in its pose and orientation belief. Instead of representing a robot's pose probability distribution within a map in a parametric form − similar to the widely-employed Kalman filter [3] −, particle filters represent this distribution by a set of samples. Their ability to incorporate motion commands and fuse them with measurements from environmental perception sensors, coupled with their above-mentioned flexibility, make them ideal for solving not only the pose tracking problem, but also the problem of global localisation.

Another way of estimating a robot's pose is scan-matching, a technique used for obtaining the relative translation and rotation between sensor poses, having the previous and the

✉ Alexandros Filotheou
alexandros.filotheou@issel.ee.auth.gr

Emmanouil Tsardoulias
etsardou@eng.auth.gr

Antonis Dimitriou
antodimi@auth.gr

Andreas Symeonidis
asymeon@eng.auth.gr

Loukas Petrou
loukas@eng.auth.gr

[1] Department of Electrical and Computer Engineering, Aristotle University of Thessaloniki, Thessaloniki, 54124, Greece

current measurements as inputs. In our context, these measurements are derived from a 2D laser range finder, and the transformation between two sensor poses is essentially the relative motion between robot poses. Scan-matching techniques have been popular with the robotics community, as they have been used in a range of applications as a form of ameliorated odometry in simultaneous localisation and mapping [4–6], local map construction [7–9], or people-tracking systems [10].

Since the pose-output of a particle filter is an estimate of its true pose and scan-matching can be used to infer the relative motion between robot poses, the two have been used in tandem so that the latter improves the former's estimate [13, 14]: range-finder measurements are used to match virtual range measurements taken from the estimated robot pose within the map of the robot's operating environment. The result of this operation may or may not be fed back to the particle filter, according to the implementation at hand.

Within the context of work, we use MCL in order to track the pose of a mobile robot over time in 2D, combined in tandem with scan-matching in order to further reduce the localisation estimate error. Scan-matching is performed *after* the particle filter has estimated the current robot pose, selected as the weight-averaged pose of a subset of all available particles, and used only for this purpose (i.e. it is not used to ameliorate the odometry or for any other purpose).

Whereas similar pose selection methods [11, 12] and tandem combinations of particle filters with scan-matching [13–15] have been explored and used in the past, our approach differs with respect to two aspects, and therefore our contribution is two-fold:

- Within the context of extracting the collective pose estimate from the set of particles from a particle filter: instead of taking its pose output to be the center of mass of the whole particle population, we study the effect that weight-averaging the pose of high-weight particles (equivalent to disregarding low-weight particles) from the total particle set has on the accuracy of the filter's estimate. This is motivated by the fact that a particle's weight is the indicator of a particle's pose estimate certainty. Our findings support our argumentation, namely that accuracy increases when low-weight particles are not considered during weight-averaging. However, and, seemingly counter-intuitively, this hypothesis collapses when the particle selection set features only one particle.
- Within the context of feeding back the (improved) pose estimate that is the result of the application of the roto-translation extracted through scan-matching a range scan from the robot's true pose and a virtual scan taken from the robot's estimated pose within the map of its environment to the filter's estimate: we study the effect that feeding back this improved pose estimate into the particle population as a collection of particles has, and juxtapose it against current state-of-the-art feedback methods. Our findings support our argumentation, namely that this method of feedback results in increased accuracy compared to all state-of-the-art feedback methods and compared also to the filter's performance when feedback is absent, and in increased robustness compared to one state-of-the-art feedback method.

The rest of this paper is structured as follows: Section 2 covers a brief review of the fundamentals of the proposed system, that is, MCL with Kullback-Leibler Divergence (KLD) sampling and scan-matching in two dimensions. Section 3 offers a comprehensive review of scan-matching techniques and their applications in assisting robot localisation. Section 4 introduces and justifies the method of selecting heavy-weight particles so as to obtain a better weight-averaged estimate from MCL. Section 5 describes how scan-matching can further assist localisation, if fitted in tandem with a localisation method. Section 6 reviews the state-of-the-art forms of feedback in tandem combinations of particle filters and scan-matching, and then introduces and justifies a method which bypasses their shortcomings. In Section 7 we formulate each one of our three claims as they were argued and justified in Sections 4, 5, and 6 in the form of hypotheses, test them by conducting simulations in two discrete environments, and present the results. Section 8 features commentary on the results, and, finally, Section 9 concludes this study.

2 Preliminaries

This section offers a brief review of the fundamental components our approach utilises towards improving the performance of particle filters via scan-matching: MCL with KLD sampling is reviewed in Section 2.1, while scan-matching in two dimensions via range scan sensors is reviewed in Section 2.2.

Before moving on to the components description, it is useful to state a classification of the localisation problems, based on their difficulty. The first and easiest problem to solve is *pose-tracking*, i.e. the robot's initial pose is a priori known and the algorithm tries to maintain a good hypothesis about the robot's pose while moving in the environment. The second problem is *global localisation*, where the initial robot's pose is unknown, and thus the algorithm has to first identify the pose and then perform pose-tracking. Finally, the third and most difficult problem is that of the *kidnapped* robot, where at some point in time of its operation the robot

is "kidnapped" – teleported elsewhere from where it was. While in global localisation the robot knows that it doesn't know where it is, in this problem the robot might think it knows where it is, while it actually doesn't; therefore it must first detect and understand this fact, and then reinitiate the global localisation algorithm.

2.1 Monte Carlo Localisation with KLD Sampling

Probabilistic approaches to the problem of robot localisation have increased accuracy and robustness compared to non-probabilistic approaches, but, depending on their nature, suffer from or solve various problems in pose estimation. For instance, Kalman filters [3] are known to be robust and accurate in the pose-tracking problem (the pose is its location and bearing within a given map), but lack the ability to represent ambiguities and to localise the robot in the case of an unknown initial pose (global localisation or kidnapped robot problems). The nature of MCL techniques [2], on the other hand, allows them to represent the uncertainty in the robot's pose by maintaining a set of hypotheses (called particles) not bound to a unimodal probability density function as in Kalman filters. Among others, this representation allows MCL approaches to globally localise a robot and keep track of pose ambiguities until being able to resolve them, by virtue of being able to represent arbitrarily complex probability densities.

Particle filters recursively estimate the posterior of a robot's pose as follows:

$$p(\boldsymbol{x}_t|z_{1:t}, \boldsymbol{u}_{0,t-1}, M) \propto \tag{1}$$
$$p(z_t|\boldsymbol{x}_t) \int_{\boldsymbol{x}'} p(\boldsymbol{x}_t|\boldsymbol{x}', \boldsymbol{u}_{t-1}) \cdot p(\boldsymbol{x}'|z_{1:t-1}, \boldsymbol{u}_{0:t-2}, M) dx'$$

Here, the pose of the robot (also called the state) at time t is denoted by $\boldsymbol{x}_t$; $\boldsymbol{u}_{0:t-1}$ is the sequence of motion commands executed by the robot, and $z_{0:t}$ is the sequence of observations made by the robot, typically obtained in contemporary robotic practices by 2D range scanners, cameras, sonars or other sensors; M is the map representing the environment in which the robot moves. The motion model $p(\boldsymbol{x}_t|\boldsymbol{x}_{t-1}, \boldsymbol{u}_{t-1})$ denotes the probability that, at time t, the robot ends up in state $\boldsymbol{x}_t$ given that it executes the motion command $\boldsymbol{u}_{t-1}$ while being in state $\boldsymbol{x}_{t-1}$ at time $t-1$. Typically, in wheeled mobile robots, motion commands are obtained via encoder sensors, and commonly referred to as *odometry*. The observation model $p(z_t|\boldsymbol{x}_t, M)$ denotes the likelihood of making the observation z_t while posed at $\boldsymbol{x}_t$. Since particle filters maintain a set of different hypotheses as to the state of the robot, each is weighed according to the likelihood that the robot measured z_t under a particle's specific pose hypothesis $\boldsymbol{x}_t^i$, where i denotes the index of particle i.

In vanilla MCL, the number of particles is fixed. To avoid divergence due to particle depletion, a large number of samples is needed so that the robot can successfully address both the global localisation and the position tracking problems [1]. This can be a severe waste of computational resources after the initial stages of localisation. KLD sampling [16] is usually employed in order for the filter to adapt the number of particles needed over time, by limiting the error introduced by the sample-based representation. The error is computed based on the Kullback-Leibler divergence between the sampled distribution and a discrete distribution computed over the whole map M. For instance, at the initial stages of localisation (when the filter is tasked to globally localise the robot) new particles are generated with larger spread, so as to cover a larger hypothesis space in M. By contrast, after the robot has successfully localised itself and the error between the above two distributions has decreased, the particle filter can maintain a smaller set of particles for tracking the robot's pose.

2.2 Scan-Matching in 2D

Scan-matching via range sensors is usually at the heart of most mapping, localisation and navigation systems, due to its ability to extract the relation between poses where distinct scans were taken. Consider a mobile robot equipped with a 2D range scan sensor, capturing two scans, z and z', the first one while the sensor is posed at $\boldsymbol{x}(x, y, \theta)$, and the second one while posed at $\boldsymbol{x}'(x', y', \theta')$, in some reference frame. These scans capture a horizontal cross-section of the environment the robot operates in. Provided that some parts of the environment are visible from both $\boldsymbol{x}$ and $\boldsymbol{x}'$, it is generally possible to find a rigid-body transformation $\boldsymbol{q}$ (also called a roto-translation) that projects the end-points of z' so that they align with those of z. This process of matching scans z and z' is called scan-matching (here in two dimensions). The solution $\boldsymbol{q}$ to a 2D scan-matching problem is comprised of two translational components, Δx and Δy, and one rotational component, $\Delta\theta$. This solution corresponds to the exact reverse motion of the robot as it travelled from $\boldsymbol{x}$ to $\boldsymbol{x}'$, or, mathematically: $\boldsymbol{x} = \boldsymbol{R}(\Delta\theta) \cdot \boldsymbol{x}' + [\Delta x, \Delta y]^\top$, where $\boldsymbol{R}(\cdot)$ is the rotation matrix operator in two dimensions. Figure 1 depicts two robot states $\boldsymbol{x}$ and $\boldsymbol{x}'$ in a rectangular environment, their corresponding range scans and the translational component of the roto-translation solution $\boldsymbol{q}$.

The operation of scan-matching (either in 2D, where its inputs are two range-scans, or in 3D, where its inputs are two 3D point-clouds) is predominantly used in robotics in inferring or correcting a robot's odometry. However, in practice, the application of $\boldsymbol{q}$ to $\boldsymbol{x}$ does not yield exactly $\boldsymbol{x}'$, due to (a) the presence of sensor noise in the input, (b) the

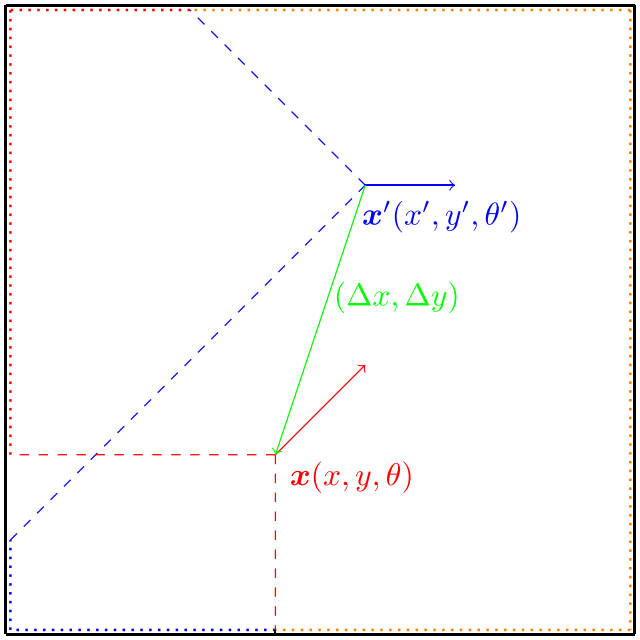

Fig. 1 The robot is initially posed at time $t = t_0$ at $\boldsymbol{x}(x, y, \theta)$, and captures a range scan $\boldsymbol{z}$. Then, at time $t_1 > t_0$, it is posed at $\boldsymbol{x}'(x', y', \theta')$, from where it captures a second range scan $\boldsymbol{z}'$. Scan-matching between $\boldsymbol{z}$ (the reference scan) and $\boldsymbol{z}'$ (the input, or "data" scan) produces the rigid-body transform $\boldsymbol{q}(\Delta x, \Delta y, \Delta\theta)$. Information pertaining to the first scan is denoted with red, while that pertaining to the second with blue. The red and blue arrows denote the robot's pose and orientation. Dashed lines depict the angular range of the scans, while dotted lines depict the parts of the environment that are visible by each scan. The colour orange is used to denote parts of the environment that are visible from both poses. The green vector depicts the translational part of $\boldsymbol{q}$, the result of scan-matching $\boldsymbol{z}$ and $\boldsymbol{z}'$

fact that a scan-matcher is not necessarily a perfect operator, and (c) the fact that a scan-matcher usually requires the tuning of several parameters, chiefs among which are the those that govern the rejection of outliers and the handling of NaN values.

For the exact mathematical expressions of the problem of 2D scan matching, and the more general problem of point registration in 3D, we refer to Censi's [17] and Besl and McKay's [18] works, respectively.

3 Literature Review

This section provides a broad review of scan-matching techniques formulated over the years (Section 3.1) and a selection of relevant applications in robot localisation (Section 3.2).

3.1 Scan-Matching Methods

Scan-matching emerged from the needs of the computer vision community with the seminal article of Besl and McKay [18], where they introduced ICP – the Iterative Closest Point algorithm, a method that determines the full six-degree spatial transformation that best aligns a free-form set of 3D points to a reference free-form point-set, according to the mean-square distance metric. In ICP, each query scan point is associated with the reference scan by identifying its closest reference scan point by means of the Euclidean distance. Once this set of correspondences is identified, ICP computes the transformation that minimises the mean-square error between the paired points. In its last step, it applies this transformation to the query scan points and updates the mean-square error. This process is iterated until the change in mean-square error falls below a preset threshold.

Lu and Milios were the first to formulate and employ scan-matching methods in order to estimate the relative translation and rotation between two robot poses by utilising 2D range sensor measurements. Although a range scan represents a 2D shape (a contour of the visible world from the robot's perspective), this shape is represented by noisy discrete points instead of a high-quality model, which makes reliably defining or extracting features difficult and possibly inaccurate [19]. In [20], two distinct algorithms are formulated that handle sensor noise and do not rely on distinguishable features in the robot's operating environment (such as lines or corners), thus avoiding the process of feature extraction and correspondence. The first method, dubbed IMPR (Iterative Matching Range to Point), considers the rotational and translational components separately, alternately fixing one and optimising the other. It is formulated as searching over a distance function to estimate the relative rotation between the input scans and using a least-squares procedure to solve for the relative translation. The second method, dubbed IDC (Iterative Dual Correspondence), yields significantly more accurate estimates of rotation than IMPR, and is based on iterative least-squares solutions, using point-to-point correspondences, similar to the ICP algorithm. Essentially, IDC combines ICP and IMPR by using ICP to calculate the translation between the two scans, and IMPR to calculate their relative rotation.

The authors of [21] were the first to extend the inclusion of uncertainty sources by developing models that account for the effects of measurement noise, sensor incidence angle and correspondence error between the environment's sensed boundary points. While they do not account for the uncertainty of the range sensor location, they incorporate the robot's odometry. A weighted range sensor matching algorithm is introduced to estimate a robot's displacement between the configurations where two-dimensional range scans are obtained, outperforming non-weighted methods, such as the algorithms of [20]. In addition, by computing the actual displacements' covariance, the weighted matching

algorithm provides the basis for optimal fusion of these estimates with odometric and/or inertial measurements, thus making it a candidate for supporting localisation and mapping tasks.

In [22] a robustified extension of ICP is introduced, dubbed TrICP (Trimmed ICP). This algorithm lifts ICP's assumption on the equality of the two input scans' sizes and, assuming knowledge of (or the ability to obtain) the minimum number of guaranteed correspondences between the two sets, it makes extensive use of the Least Trimmed Squares method [23] in order to enhance ICP's loop of execution. ICP is found to be a special case of TrICP if both sets have the same size and all points from both sets can be paired with one-another.

Biber and Strasser introduced the Normal Distributions Transform (NDT) in [24], in an effort to support the task of robot map-building. Assuming 2D range scans as inputs, NDT regularly subdivides the 2D plane, similar to an occupancy grid; but where the occupancy grid represents the probability of a cell being occupied, NDT represents the probability of measuring a sample point of a range scan for each position *within* the cell itself. The result of the transform is a piecewise continuous and differentiable probability density that can be used to match another scan, here using Newton's algorithm [25]. The advantages of this way of representation are that (a) all involved derivatives can be analytically, quickly and correctly calculated, and, most importantly, (b) that no explicit correspondences (either between features or points) between any two scans have to be established, thereby reducing the degree to which all scan-matching methods are prone to error. The relative translation and rotation between an input and a reference scan are iteratively computed by maximising (via performing one step of Newton's algorithm) a score function, being the sum of evaluation of all distributions of the input scan mapped to the frame of reference of the first scan, based on an initial estimation of them (for example taken from odometric readings).

Scan-matching for global robot localisation has been explored in [26]. Assuming that a robot's operating environment is structured and that line segments are prevalent in it, the authors' algorithm, dubbed CLS (Complete Line Segments), matches complete line segments extracted from input range scans to complete line segments extracted from the map representing the robot's operating environment, thus providing an accurate way of extracting the robot's global position in the map.

In [27], the authors extend the applicability of scan-matching to global and local localisation (position tracking). By transferring the problem of scan-matching to the Hough domain, they exploit several of its properties: namely that no information is lost in the process and that invariance allows them to decouple the problem into initially finding the orientation error, followed by the translation error. The HSM (Hough Scan Matching) algorithm is a global, multi-modal, non-iterative scan-matcher that can operate in unstructured environments. Contrary to CLS, HSM does not rely on features' extraction, but matches dense data, i.e. range scan measurements that can be interpreted as distributions of features in a different convenient parameter space, allowing HSM to match non-linear surfaces while making the process robust to sensor noise.

In [28], the authors present a probabilistic method for matching 2D range scans obtained in unstructured environments. While their algorithm, pIC (probabilistic Iterative Correspondence), is designed to handle the input sensor's noise, in contrast to [21], it is also able to handle the range sensor pose uncertainty. pIC follows a two-step process, whereby it probabilistically identifies correspondences between two input scans and then it simultaneously captures their relative translation and rotation. Experiments against ICP and IDC indicate a faster convergence in the task of localisation, while improving on ICP and, in the task of mapping, it is shown that pIC outperforms both in terms of robustness, accuracy and convergence.

Contrary to the aforementioned methods, the authors of [29] advocate that it is advantageous for a matching algorithm to operate in the laser scan's native polar coordinate system. Their method, Polar Scan Matching (PSM), belongs to the family of point-to-point matching approaches. It avoids the search of point associations by matching similar bearing points, by alternating between scan projection followed by translation estimation and scan projection followed by orientation estimation. In experiments, PSM is shown to be computationally faster than ICP, both in terms of iterations and processing time, as well as in terms of accuracy.

A new distance function is introduced in [30], suitable for robot poses in the (x, y, θ) space: the distance between two poses is the smallest rigid body transformation that leads one pose to the other. This distance measure is employed in both steps of their algorithm, dubbed MB-ICP (Metric-Based Iterative Closest Point): points from an input 2D range scan are initially matched to those of a reference scan, and then the relative translation and rotation between the two scans is concurrently computed, thanks to the distance measure's incorporation of displacement in terms of spatial and angular distance, by iteratively minimising the least-square error of this new measure with respect to matched points. With this formulation, the authors are able to improve on IDC in terms of robustness, convergence speed and precision.

Censi, motivated by the fact that reasonable correspondences between the two input 2D range scans may not exist – since the range sensor sparsely samples the environment

and hence different scans may sample different parts of it −, instead of using a point-to-point metric for distance, uses a point-to-line one in [17], where PL-ICP (Point to Line Iterative Closest Point) is introduced. The upside of using a point-to-line distance metric is that a closed form for the minimisation of this metric can be found, thereby increasing the accuracy and speed of convergence of matching. Indeed, the resulting algorithm converges quadratically (whereas ICP converges linearly) and in a finite number of steps. PL-ICP is compared against ICP, IDC and MB-ICP and is found to be superior in accuracy, number of iterations required to converge (more than three times as low), and execution time (more than 40 times as low). The intuitive explanation behind this increase in accuracy is that the point-to-line metric approximates the real surface distance better than the point-to-point metric. However, especially opposed to MB-ICP, PL-ICP is susceptible to large initial displacement errors and, in particular, in large angular errors.

Olson [31] advocates that modern computing machinery is computationally fast enough for scan-matching methods to move on from heuristic methods to more exact ones. Indeed, the bulk of scan-matching methods use imperfect and susceptible to initial weak priors heuristics to quickly compute the optimum alignment of two input scans, rather than focus on quality first and then execution speed. He argues that scan-matching is rarely convex when viewed as an optimisation problem, with the surface of the cost function involved having many local minima, thus making a local optimiser susceptible to being trapped therein, while making it harder to locate its global minimum. In [31] a probabilistic scan-matching algorithm is formulated that produces higher-quality results at the cost of additional computation time, although this method is able to run in real-time. Rather than trusting a local search algorithm to find the global maximum (the rigid-body transformation that maximises the probability of having observed the input 2D scan), the proposed algorithm performs a search over the entire space of plausible rigid-body transformations. This region is derived from a prior which in turn can be derived from odometric measurements. The correlation-based method presented is shown to be very accurate and robust to uncertainty in the sensor's location.

Perimeter-based polar scan matching (PB-PSM) [32] is a technique based on [29] that favors matches with a larger perimeter overlap between the two input scans, while using a robust cost minimisation process, namely an adaptive direct search method, made possible due to a linear complexity data association technique. Contrary to other methods, an initial guess is not required as input, although, if one is provided, it results in increase of robustness and decrease of computational requirements. The input scans are first filtered, then searched for data associations, and finally a cost function is built from the associated point pairs. The cost is proportional to the overlap between the scans and the best solution is found by minimising the cost using a form of exhaustive search. The minimisation process is performed for rotation first, followed by translation, and the process is iterated until adequate convergence is achieved.

Finally, the authors of [33] developed a method to extract the roto-translation between two input range scans by building a correlation function that reflects the degree of their alignment according to some argument roto-translation. The latter is naturally extracted by maximising the said function. Their method has low computational requirements and is targeted at the embedded low-power devices typically found in mobile robot platforms. Compared to ICP, it is approximately 10 times faster, and it has a wider operating range; however, the obtained transformation vectors suffer from a relatively rough resolution and slightly higher relative errors.

3.2 Scan-Matching in Robot Localisation

A localisation method based on 2D range scan matching is described in [34], where a simple stochastic search algorithm is employed to correct the robot's pose due to its inevitable odometric drift. This auxiliary localisation behaviour is activated whenever an error measure is found to be above a preset threshold. This error measure is in turn based on the relative deviation in detected distances between rays of the robot-mounted range scan and a virtual scan − essentially the output of ray-casting on the map of the robot's operating environment from the estimated laser sensor's pose across the same number of rays as those of the physical range sensor. To avoid having to correct for the motion of the robot while scan-matching, the robot is assumed to be standing still for the whole duration of its pose correction. Therefore, whenever the error measure is found to be above its preset threshold, the algorithm halts the robot's motion, and picks a random pose in the neighbourhood of its estimated pose. It then takes a virtual range scan from that pose, and computes the new error. If the error is lower than the one found for the previous estimated pose, a new iteration starts, this time centered around the newly found pose; if not, the algorithm keeps guessing poses until it finds one whose error is lower than the previous one. The final pose is then taken as the true pose of the robot, allowing a correction of the odometry.

The authors of [35] use scan-matching to improve the solution of the global localisation problem. For identifying the robot's global pose, and assuming that the robot's environment is structured and without any sort of symmetries, they employ HSM [27] to obtain the robot's heading by matching the lines in the map of the environment with the lines from the 2D range scan taken at the robot's initial pose. Having found the robot's orientation, they

estimate the robot's location by calculating the likelihood that each location on the map's grid produced the input laser scan using the beam endpoint model [1], and extract the one with the maximum probability. As for pose tracking, just like in [36], they replace the robot's odometry – due to its noisy nature and the particle filter's need of large particle population to adequately sample from the proposal distribution (which is based on odometric readings) – with motion estimates extracted from consecutive range scans using ICP, due to their range sensor's superior accuracy and resolution compared to odometry.

Focusing on industrial applications of mobile robotics, the authors of [15] achieve millimeter accuracy at predefined taught-in locations using a combination of particle filters [2], KLD sampling [16] and scan-matching. They argue that the limited number of particles typically used in particle filters and the relatively coarse resolution of the occupancy grid map used to represent a robot's operating environment results in pose estimates that do not satisfy the needs of industrial applications and, in order to improve them at specific a priori known locations, they store local range scan measurements as reference observations in the map, and use these at runtime for scan-matching. This method, contrary to [34], has the advantage of not being limited by the map's limited fidelity and resolution. They use Censi's PL-ICP [17] to match the scans obtained at runtime to the reference scans, and MCL's estimate as its initial guess input. The whole localisation regime operates in open-loop, meaning that the result of scan-matching is not integrated or fed-back in any way to MCL.

Scan-matching has been also employed in appearance-based navigation tasks [37, 38], which do not necessarily need to rely on a map of the environment and can directly operate in the space of sensor data. In [39], the authors use PL-ICP to perform localisation relative to a pre-recorded taught trajectory, represented as a sequence of anchor points, consisting of raw odometry readings and 2D range data. Bypassing the limited fidelity and resolution of a map of the environment, they also achieve millimeter accuracy, but, contrary to [15], across precomputed anchor points on the taught-in trajectory, outperforming MCL in the task of teach-and-repeat.

In [13], the authors make use of a pipeline scheme, combining MCL, KLD, PL-ICP and the concept of virtual scanning similarly to [34]: every time the particle filter outputs its estimate of the robot's pose, a virtual 2D range map scan is taken from that pose and fed to PL-ICP together with the latest real 2D range scan. The roto-translation of the former with regard to the latter is applied to the pose estimated by MCL, and this pose is in turn used to re-initialise MCL, therefore forming a closed loop. Although this form of loop-closure is very strict, as any significant error in scan-matching will result in severe error in pose estimation, the authors do not report such errors arising, and record a mean location error with a 2-norm around 1.6 cm and a mean orientation error of 0.13°. This localisation regime is evaluated in industrial settings and its performance is rigorously and repeatedly evaluated at specific and predetermined locations.

The authors of [14] employ a similar pipeline: they use a 2D range scan matching method to align a virtual map scan measurement to a physical range sensor measurement using the Gauss-Newton method during their optimisation of scan-alignment, but do so layer-by-layer in increasing map resolution. The resulting improved pose is fed-back to MCL, not as its initial condition this time, but as a new particle in its population. They experimentally evaluated their method with a real robot and show that their method is able to achieve a mean location error with a 2-norm around 1.1 cm and a mean orientation error of 1.1° throughout the robot's navigation.

4 Pose Selection in Particle Filters

Assuming a mobile robot operating in the 2D plane, particle filters maintain the estimate of a robot's pose at every time step t, $\hat{\boldsymbol{x}}_t(x, y, \theta)$, within a map M, in the form of a set of "particles", i.e. randomly drawn samples from the probability distribution $p(\boldsymbol{x}_t|\boldsymbol{z}_t, M)$, where $\boldsymbol{z}_t$ is a vector of observations, sensed at time t by the robot through the use of its sensor(s), which, for simplification reasons, is comprised solely of one 2D range scanner. The representation of the distribution $p(\boldsymbol{x}_t|\boldsymbol{z}_t, M)$ by a set of samples is due to the essential duality between the former and the latter [40].

This quality of particle filters allows them to be able to represent multi-modal distributions – a precondition for global localisation – but, by the same token, providing a definitive answer to the question of combining all possible hypotheses (each particle expresses a discrete hypothesis about the robot's state within M) and computing a unified estimate of the robot's pose is made ambiguous: in Kalman filters for instance, which are strictly unimodal estimators, by contrast, the filter's mean estimate of the pose vector and covariance matrix suffice to compute the estimate of $\boldsymbol{x}_t$ [3], whereas in particle filters there is no single closed-form solution to this problem. The prevailing approach to computing the estimated pose and its variance is implicit, and it assumes identifying within the distribution of particles the mode with the highest total weight, calculating its center of mass, and then calculating the variance around it. In the case where the estimate has converged and the distribution has become unimodal, this approach is equivalent to averaging *all* particles' estimates according to their individual weight.

The literature on extracting or surmising the final pose off of a particle filter based on some particular particle

characteristics is rather thin: [11] and [12] focus on humanoid robots in the context of robotic soccer; first, at time t they identify the particle within certain translational and rotational distance bounds to the estimate of the pose at time $t-1$ with the highest weight. The authors perform selection in this fashion in order to mitigate pose discontinuity. Then, if the weight of the cluster of the identified particles is not small, the end pose is calculated as the centroid of all particles within a preset radius of this particle; however, if it is "small", only the particle with the highest weight is reported. In what follows we demonstrate that this latter decision, while intuitive, is actually not wise, and therefore not a viable candidate for extension to other conditions and situations other than in the context of these two works.

In particle filters, each particle is associated with an importance factor, or weight. The weight w_t^i of a particle i at time t quantifies a robot's probability of having observed the actual measurements $\boldsymbol{z}_t$ from that particle's estimated pose $\hat{\boldsymbol{x}}_t^i(x_i, y_i, \theta_i)$. This means that, given a map M of fidelity to the robot's operating environment, the more accurate the estimate of the robot's pose is, the more close $\hat{\boldsymbol{x}}_t^i(x_i, y_i, \theta_i)$ is to the robot's true pose $\boldsymbol{x}_t(x, y, \theta)$, and therefore the higher the probability that the actual measurements $\boldsymbol{z}_t$ and the predicted measurements $\hat{\boldsymbol{z}}_t^i$ agree with each other is. Therefore, in theory, a direct disproportionality exists between the estimate error (the deviation of the estimated pose from its true value) of a particle and the value of its weight: the lower its pose estimation error, the higher its weight, and vice-versa.

This final inference, juxtaposed against the dominant approach in inferring the filter's estimate, served as our motivation behind exploring pose-extraction methods other than the prevailing one. Theoretically then, we would expect that selecting high-weighted particles (which is equivalent to discarding low-weight particles − particles whose pose estimate explains measurements $\boldsymbol{z}_t$ in a more unsatisfactory manner compared to other particles in the population) for calculating the compound estimate of the filter, would result in better pose estimates, that is, pose estimates closer to the true value of the robot's pose at every time step. Since the weight of a particle is a defined, quantifiable and definitive measure of alignment of sensor inputs and expected sensor inputs conditioned on the particle's pose estimate, and value is bestowed upon a particle's weight in a proportional manner, all selection methods we shall cover are weight-based methods. We confine our selection methods to weight-based approaches since in the context of particle filters the weight of a particle is the sole indicator of its quality of estimate.

Let us denote by $\boldsymbol{P}_t$ the entirety of the population of particles at time t. Then $\boldsymbol{P}_t \equiv \{(\hat{\boldsymbol{x}}_t^i, w_t^i)\}, i = 0, 1, \ldots, |\boldsymbol{P}_t| - 1$, where $\hat{\boldsymbol{x}}_t^i$ is the estimate of the i-th particle of the robot's pose at time t, and w_t^i is the weight associated with particle i at time t. Furthermore we denote by $\overline{W}_t = \frac{1}{|\boldsymbol{P}_t|} \sum_{i=0}^{|\boldsymbol{P}_t|-1} w_t^i$ the mean weight of particles in $\boldsymbol{P}_t$. Then we distinguish two discrete selection methods: (a) absolute and (b) relative selection methods. In absolute selection methods, an absolute percentage or number of particles of the population $\boldsymbol{P}_t$ is called to vote for the pose estimate at time t. The prevailing pose calculation method is a special case of absolute selection, where the percentage of selected particles is 100%. In relative selection methods, particles are chosen to vote conditioned on the relation of w_t^i and $\overline{W}_t$: for example, only particles whose $w_t^i > \overline{W}_t$ are chosen to have a say in the filter's overall pose estimate. Algorithm 1 illustrates the process of particle selection.

Algorithm 1 `particle_selection`.

Input: $\boldsymbol{P}_t \equiv \{(\hat{\boldsymbol{x}}_t^i, w_t^i)\}$, selection_manner, fraction
Output: pose estimate $\hat{\boldsymbol{x}}_t$

1: **assert** selection_manner = ABSOLUTE | | RELATIVE
2: **assert** fraction $\in [0, 1]$
3: **if** selection_manner = ABSOLUTE **then**
4: $\quad \boldsymbol{P}'_t \leftarrow$ sort $\boldsymbol{P}_t$ by weight w_t^i, descending
5: $\quad$ **if** fraction > 0.0 **then**
6: $\quad\quad \boldsymbol{P}''_t \leftarrow \boldsymbol{P}'_t[0 : \lfloor \text{fraction} \cdot |\boldsymbol{P}'_t| \rfloor - 1]$
7: $\quad$ **else**
8: $\quad\quad \boldsymbol{P}''_t \leftarrow \boldsymbol{P}'_t[0]$
9: $\quad$ **end if**
10: **end if**
11: **if** selection_manner = RELATIVE **then**
12: $\quad \overline{W}_t \leftarrow \frac{1}{|\boldsymbol{P}_t|} \sum_{i=0}^{|\boldsymbol{P}_t|-1} w_t^i$
13: $\quad \boldsymbol{P}''_t \leftarrow \hat{\boldsymbol{x}}_t^i : w_t^i > \overline{W}_t$
14: **end if**
15: $\hat{\boldsymbol{x}}_t \leftarrow (0, 0, 0)$
16: **for** $j = 0 : |\boldsymbol{P}''_t| - 1$ **do**
17: $\quad \hat{\boldsymbol{x}}_t \leftarrow \hat{\boldsymbol{x}}_t + \boldsymbol{P}''_t[j].w_t^i \cdot \boldsymbol{P}''_t[j].\hat{\boldsymbol{x}}_t^i$
18: **end for**
19: **return** $\hat{\boldsymbol{x}}_t$

In Algorithm 1, if absolute selection is chosen, the particle population is first sorted by weight (line 4) in a descending order. Then the first $\lfloor \text{fraction} \cdot |\boldsymbol{P}'_t| \rfloor$ particles are chosen to be carried forward, where fraction $\in [0, 1]$ expresses the proportion of particles to be considered (line 6); the convention fraction $= 0$ is reserved for selecting the particle with the highest weight among those of $\boldsymbol{P}_t$. The notation $\boldsymbol{P}'_t[a]$ for particle set $\boldsymbol{P}'_t$ denotes the particle of $\boldsymbol{P}'_t$ at index a; the notation $\boldsymbol{P}'_t[a{:}b]$ denotes the set of particles constituted by the elements of $\boldsymbol{P}'_t$ from index a up to index b. On the other hand, if relative selection is chosen, the population's mean weight is calculated first (line 12), and then all particles whose weight exceed this threshold

are included in the particle set carried forward (line 13). In both cases the pose hypotheses of the particle set holding selected particles, $\boldsymbol{P}''_t$, are then weight-averaged (line 17) and the resulting pose is considered the output of particle selection. The notation $\boldsymbol{P}''_t[j].x$ for particle set $\boldsymbol{P}''_t$ denotes the x component of the element of $\boldsymbol{P}''_t$ at index j.

One justifiable question/censure that can be raised is why not keep the total population size to the selection fraction and dispense with the selection mechanism altogether. This would potentially be catastrophic, as keeping a lower number of particles would increase the risk of particle deprivation [1]: as the population size increases, so does the fidelity of the posterior (1) to the true pose; conversely, the lower the number of particles in the filter the larger the probability of the filter's divergence. Thus, it is reasonable to guard against particle deprivation with an increased population size and employ a selection regime so that the system increases its accuracy without sacrificing posterior quality/accuracy or the stability of MCL.

Although in theory the above selection methods are sound (in that selecting heavier particles, thus discarding poor-estimate particles, improves the quality of the overall estimate), in practice (Section 8.1) we observe varying or adverse results, which may be attributed to (a) the loss of overall information, (b) the higher degree of influence particles obtain when the cardinality of the voting set is decreased, and/or (c) the removal of near-symmetrically-posed particles, present in the population due to the randomness introduced during the filter's prediction phase.

In the next section we reason how the gap between the estimated pose of MCL and the true pose can be further reduced by means of scan-matching.

5 Improving the Localisation Estimate Via Prosthetic Scan-Matching

In the current study we seek to improve the estimate of a particle filter by various means: in the previous section we theoretically reasoned about how selecting heavy-weighted particles for determining the filter's output pose poises the filter into calculating more accurate estimates. In this section we will review how scan-matching can be employed as a prosthesis of particle filters (or any other localisation technique in fact) so that the final system's estimates fall closer to the truth. This technique is inspired from [13] and is covered in greater detail here for purposes of thoroughness and completeness.

Suppose that a robot equipped with a 2D range scanner operates in a set environment which is represented via an occupancy grid map M. Suppose also that at time t the particle filter outputs an estimated pose $\hat{\boldsymbol{x}}_t(x, y, \theta)$ using some selection method, and that a range scan, captured from the true pose of the robot, L_t^R, is also available at time t. Then, if we construct a virtual scan L_t^V, which is the output of a ray-casting operation originating at $\hat{\boldsymbol{x}}_t$ that simulates the operating principle of the real range scanner *but this time on the map* M across the same angular range, it is possible by scan-matching the two range scans (Section 2.2) to obtain the roto-translation $\boldsymbol{q}_t$ which, if applied to the estimate $\hat{\boldsymbol{x}}_t$, will make it coincide with the true pose $\boldsymbol{x}_t$. In this context, L_t^R is considered to be the reference scan, and L_t^V the input, or data, scan.

However, due to (a) the presence of sensor noise in L_t^R, (b) the inevitable mismatch between the operating environment and its map M, (c) its discrete nature (M is assumed to be a grid map of finite resolution), and (d) the fact that the scan-matcher employed is not necessarily perfect, we expect that what actually happens is that the application of $\boldsymbol{q}_t$ to the pose estimate $\hat{\boldsymbol{x}}_t$ will move this estimate in *a vicinity* of the true pose rather than exactly to it. This estimation error depends on a multitude of parameters, among others, namely the quality of the robot's odometry, the match of its kinematic model with its actual dynamics, the amount of sensor noise, the map's resolution, the scan-matchers accuracy in translation and rotation estimation, the size of the particle population, the layout of the map coupled with the scan-matcher's ability to reject outliers, and the maximum range of the range scan sensor.

Depending on the configuration of MCL, we would like to employ a scan-matcher that is able to keep up with the frequency of pose updates, that is, to operate in real time. The scan-matching technique of our choice is PL-ICP [17] due to the following reasons: (a) it surpasses the de facto state-of-the-art in precision, number of iterations until convergence and average execution time, and (b) it requires less tuning parameters, as it requires neither error thresholds for halting convergence nor maximum estimates of the initial guess.

6 Improving the Overall System's Estimate Via Feedback

Although the localisation estimate output by the scan-matching technique $\hat{\boldsymbol{x}}'$ suffers from the above sources of error, it is, in principle, more accurate than that output by MCL, $\hat{\boldsymbol{x}}$. What this means is that the overall tandem system holds an estimate of which MCL is not informed. Thus, it would be advantageous to input $\hat{\boldsymbol{x}}'$ into MCL and, in the literature, this is accomplished by two methods:

- The first way of feeding back $\hat{\boldsymbol{x}}'$ to MCL is to initialise it with this estimate. This means that the particle population maintained by the filter is created anew, with particles being dispersed around $\hat{\boldsymbol{x}}'$ with a preset

variance. This is the approach followed in [13], and will be referred to in the rest of this work as **hard loop-closure**.

- The second way is to inject the particle population with one particle, representing the estimate $\hat{\boldsymbol{x}}'$, serving as one discrete hypothesis among the current population. This is the approach followed in [14], and will be referred to as **soft-1 loop-closure**.

One of the concerns that can be raised about hard loop-closure is that it is not robust to localisation failures: if the pose output by scan-matching is erroneous, then the entirety of MCL's population will be initialised around that pose, with a catastrophic effect on localisation. Furthermore, with regard to soft-1 loop-closure, injecting one particle over a minimum population of several hundred takes longer times to have an effect than if a larger portion of the population was substituted for the improved estimate. Thus, the more particles are inserted into the population the more accelerated and improved its convergence would be (with reservation for the case where *all* particles are substituted for multiple copies of the same pose estimate; the precariousness of this approach lies in the absence of the filter's variance).

Motivated by the above facts, we introduce a hybrid loop-closure strategy, where the estimate $\hat{\boldsymbol{x}}'$ is injected into the particle population as *a plethora of particles*. Their proportion to the total final population is fixed and set beforehand. Here, supposing that the maximum population size is N_{max}, that the desired injected population size compared to the population size after its injection is $q \in (0, 1)$, and that at time t the population size is N_t, we distinguish three cases:

- $N_t = N_{max}$
  When the population is at its maximum capacity, particles are sorted by descending weight, and the lower $\lfloor qN_{max} \rfloor$ particles are deleted, giving way to the introduction of an equal number of particles, all clones of $\hat{\boldsymbol{x}}'$. It is obvious that $qN_{max}/N_{max} = q$.
- $N_t \leq (1-q)N_{max}$
  In this case, no particles are deleted, and $\frac{q}{1-q}N_t$ particles are added. It is easy to see that

$$\frac{\frac{q}{1-q}N_t}{\frac{q}{1-q}N_t + N_t} = \frac{qN_t}{qN_t + (1-q)N_t} = \frac{qN_t}{N_t} = q$$

- $(1-q)N_{max} < N_t < N_{max}$
  In this case, the population of particles N_t is sorted by descending weight, the lower $\lfloor N_t - (1-q)N_{max} \rfloor$ particles are deleted, and $\lfloor qN_{max} \rfloor$ copies of the hypothesis extracted from scan-matching are introduced into the population. Again the population introduced is, as a proportion, q times the final population size:

$$\frac{qN_{max}}{N_t - (N_t - (1-q)N_{max}) + qN_{max}} = \frac{qN_{max}}{N_{max}} = q$$

The proposed feedback strategy (a) can steer the system away from the pitfall of faulty pose estimates output by scan-matching – something unavoidable by the approach of hard loop-closure – by not replacing the totality of particles in MCL's population, but instead keeping a portion of its best estimates (best in the sense of higher-weighted) from one filter iteration to the next so that, even if scan-matching outputs a spurious estimate, the filter can recover by virtue of maintaining past estimates residing in the vicinity of the true pose, and (b) accelerates convergence by inserting not one particle – as in the case of soft-1 loop-closure method –, but a multitude of better-estimate particles.

The proposed feedback strategy will be referred to hereafter as **soft-*p* loop-closure**, where p is expressed in percentage terms (e.g. in the regime of soft-50 loop-closure, every time MCL outputs a result to PL-ICP, the latter improves its estimate and introduces – and possibly deletes – as many particles as needed so that the final proportion of copies of its output is 50% of the particle filter's final total population; the term soft-1 loop-closure will be reserved for reference to the original idea of inserting only one particle to the filter's population).

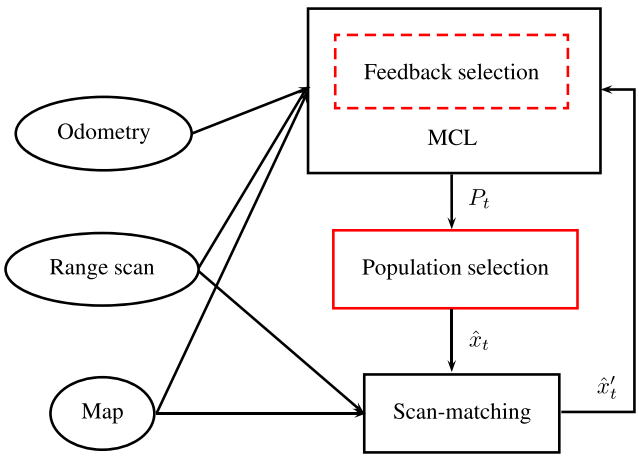

Fig. 2 The overall system in block structure. Blocks indicate subsystems, while ellipses indicate their inputs. The colour red is used to identify the contributions of our approach to the state-of-the-art in tandem systems of particle filters and scan-matching. Here, scan-matching is treated as a prosthesis of MCL. MCL's population $\boldsymbol{P}_t$ is subject to weight-based selection at time $t > 0$. The selected particles are weight-averaged and the resulting pose is used as the origin of a virtual scan across the map. The real and virtual scans are then matched using PL-ICP. The output of scan-matching $\hat{\boldsymbol{x}}'_t$ is, in principle, more accurate than that of MCL, $\hat{\boldsymbol{x}}_t$, which means that it could be used to serve in assistance to MCL's localisation by feeding it back to it. See text for the three ways that feedback can be introduced in particle filters

The structure of the compound system is depicted in Fig. 2. The algorithmic form of the feedback mechanism is illustrated in Algorithm 2 and the mechanism's conceptual content is depicted in block form in Fig. 3.

Algorithm 2 `feedback_selection`.

Input: $\boldsymbol{P}_t \equiv \{(\hat{\boldsymbol{x}}_t^i, w_t^i)\}$, q, $\hat{\boldsymbol{x}}_t'$, feedback_manner
Output: $\boldsymbol{P}_{t+1}$

assert feedback_manner $\in$ {HARD, SOFT_1, SOFT_P, OPEN }
if feedback_manner = HARD **then**
  $\boldsymbol{P}_{t+1} \leftarrow \overbrace{\{\hat{\boldsymbol{x}}_t'\} \cup \{\hat{\boldsymbol{x}}_t'\} \cup \ldots \{\hat{\boldsymbol{x}}_t'\}}^{N_{max}}$
  Perturb $\boldsymbol{P}_{t+1}.\hat{\boldsymbol{x}}_t^i$ according to MCL init params
end if
if feedback_manner = SOFT_1 **then**
  if $|\boldsymbol{P}_t| = N_{max}$ **then**
    $\boldsymbol{P}_t \leftarrow$ Sort $\boldsymbol{P}_t$ by weight, ascending
    Delete $\boldsymbol{P}_t[0]$
  end if
  $\boldsymbol{P}_{t+1} \leftarrow \boldsymbol{P}_t \cup \hat{\boldsymbol{x}}_t'$
end if
if feedback_manner = SOFT_P **then**
  assert $q \in (0, 1)$
  $\boldsymbol{S} \leftarrow \{\}$
  if $|\boldsymbol{P}_t| \leq (1-q)N_{max}$ **then**
    $\boldsymbol{S} \leftarrow \underbrace{\{\hat{\boldsymbol{x}}_t'\} \cup \{\hat{\boldsymbol{x}}_t'\} \cup \ldots \{\hat{\boldsymbol{x}}_t'\}}_{\left\lfloor \frac{q}{1-q} |\boldsymbol{P}_t| \right\rfloor}$
  else if $|\boldsymbol{P}_t| = N_{max}$ **then**
    $\boldsymbol{P}_t \leftarrow$ Sort $\boldsymbol{P}_t$ by weight, ascending
    Delete $\boldsymbol{P}_t[0 : \lfloor qN_{max} \rfloor - 1]$
    $\boldsymbol{S} \leftarrow \underbrace{\{\hat{\boldsymbol{x}}_t'\} \cup \{\hat{\boldsymbol{x}}_t'\} \cup \ldots \{\hat{\boldsymbol{x}}_t'\}}_{\lfloor qN_{max} \rfloor}$
  else
    $\boldsymbol{P}_t \leftarrow$ Sort $\boldsymbol{P}_t$ by weight, ascending
    Delete $\boldsymbol{P}_t[0 : \lfloor |\boldsymbol{P}_t| - (1-q)N_{max} \rfloor - 1]$
    $\boldsymbol{S} \leftarrow \underbrace{\{\hat{\boldsymbol{x}}_t'\} \cup \{\hat{\boldsymbol{x}}_t'\} \cup \ldots \{\hat{\boldsymbol{x}}_t'\}}_{\lfloor qN_{max} \rfloor}$
  end if
  $\boldsymbol{P}_{t+1} \leftarrow \boldsymbol{P}_t \cup \boldsymbol{S}$
end if
if feedback_manner = OPEN **then**
  $\boldsymbol{P}_{t+1} \leftarrow \boldsymbol{P}_t$
end if
return $\boldsymbol{P}_{t+1}$

In Algorithm 2, if hard-closed-loop is selected as the method of feedback, the particle set is filled with N_{max} copies of the system's output at the previous timestep and then each component of each particle's pose hypothesis is subject to minor disturbance according to parameters

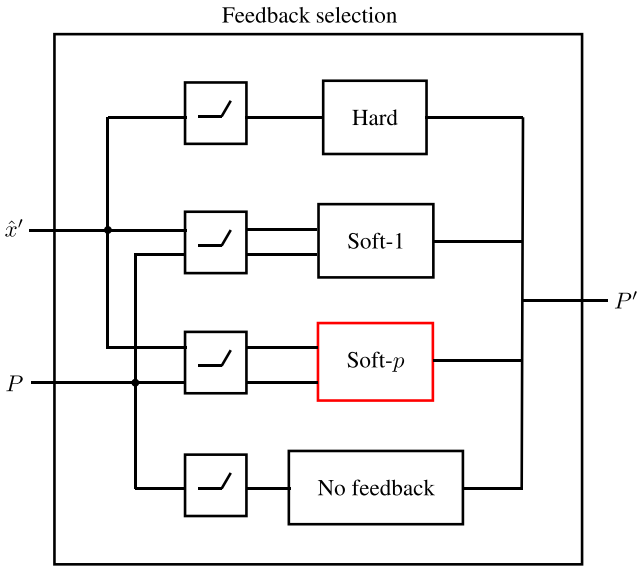

Fig. 3 Internal to the modified version of MCL, there are 4 distinct and mutually exclusive modes of feedback. Denoting by $\hat{\boldsymbol{x}}'$ the output of the scan-matching process, by $\boldsymbol{P}$ the filter's population at the time of feedback execution, and by $\boldsymbol{P}'$ the population output by feedback: (**a**) hard loop-closure, where the population of MCL is initialised anew, with $\boldsymbol{P}'$ comprised of particles spread around $\hat{\boldsymbol{x}}'$, (b) soft-1 loop-closure, where $\hat{\boldsymbol{x}}'$ is introduced into $\boldsymbol{P}$ in the form of one discrete particle, (**c**) soft-p loop-closure, where $p\%$ of $\boldsymbol{P}'$ is comprised of clones of one particle with pose equal to $\hat{\boldsymbol{x}}'$ and $(100-p)\%$ is comprised by the corresponding in number heavy-most particles of $\boldsymbol{P}$, and (**d**) no feedback at all. The colour red is used to identify the contribution of our approach with respect to feedback methods to the state-of-the-art in tandem systems of particle filters and scan-matching. Feedback modes are immutable and set a priori

internal to MCL (the same process taking place when providing vanilla MCL with an estimate of the robot's pose). If soft-1 loop-closure is selected, the system's output is inserted into the population as one pose hypothesis, either by replacing its lowest-weighted particle when the population is at its maximum, or by direct insertion otherwise. If soft-p loop-closure is selected, particle set $\boldsymbol{S}$ is filled with as many copies of the system's output as needed so that after insertion their proportion over the entire population is q (or $p = 100q\%$). In open-loop the population undergoes no modification. Signifiers "HARD", "SOFT_1", "SOFT_P", and "OPEN" are shorthand for the four admissible modes of feedback, namely hard loop closure, soft-1 loop closure, soft-p loop closure, and no feedback, respectively.

The introduced overall system is more flexible than a tandem combination of vanilla MCL with KLD sampling and scan-matching, as the latter is a specific case of the former: selecting 100% of the particles from the population of MCL for extracting its pose estimate and no feedback makes the overall system devolve into the simplest case of configuration of the introduced system, i.e. what is now considered MCL with KLD sampling. Furthermore,

both approaches presented in [13] and [14] are special configurations of the proposed system.

In the following, when we refer to the pose output by MCL we refer to $\hat{\boldsymbol{x}}_t$, and when we refer to the pose output by the system, or the compound system, or the overall system, we refer to $\hat{\boldsymbol{x}}'_t$.

7 Simulations and Results

The content of this section serves the testing of three discrete hypotheses, as articulated in Sections 4, 5, and 6:

(H1) Selecting high-weighted particles from the population of MCL − equivalently: discarding low-weight particles from it − and averaging their weighted poses results in increased pose accuracy compared to selecting all particles from the population and averaging their weighted poses;

(H2) Scan-matching between (a) a scan obtained through the physical range-finder sensor of the robot and (b) a virtual scan obtained through ray-casting the map in which the robot navigates from its estimated pose and applying the resulting roto-translation to MCL's pose estimate results in increased pose accuracy compared to vanilla MCL when feedback is absent;

(H3) Feeding back the (hypothesised improved) roto-translated pose acquired through the application of the result of the above scan-matching process to the pose estimate of MCL in the form of a group of particles comprising $p\%$ of the final particle population, where p is sufficiently lower than 100 and larger than 1, (a) results in increased pose accuracy compared to vanilla MCL, (b) results in increased pose accuracy compared to feeding-back only one particle with such corrected pose, and (c) is more robust than initialising MCL anew around the roto-translated pose.

In the third hypothesis we refer to robustness in the sense of the ability of a system to *avoid* failure, rather than *recover* from failure, referred to as "resilience" [41, 42], as the latter is a property of a particle filter itself, whereas the ability to avoid failure (in this case reinitialisation around a catastrophically erroneous pose) is a property of the feedback method.

These hypotheses are tested on two discrete simulated environments. Due to our group's investigation of the problem of localisation of RFID-tagged objects [43, 44], these environments were selected and constructed as such in order to reflect the conditions in which we expect that RFID-tagged objects will be placed in the real world. Naturally, accurate robot localisation is a condition for accurate localisation of RFID tags: the more accurate the estimate of the robot's pose is the more accurate the position of the tags on the map will be.

The two environments are dubbed CORRIDOR, denoted by M_C and presented in Fig. 4, of size 10×7 m^2, and WAREHOUSE, denoted by M_W and presented in Fig. 5, of size 20×42 m^2. The resolution of both maps is 0.01m×0.01m/cell. The former is used to illustrate the efficacy of the proposed system in non-complex environments, where all of its boundaries are within the range of the robot's 2D range sensor at all times. By contrast, the latter is a large warehouse, −the natural habitat of RFID-tagged objects in industry− intended to put more strain on the system and thus its performance: obstacles are further apart than in CORRIDOR, which means that either not all rays of the sensor carry valuable and usable information, or they are more corrupted by noise, as the range error increases with the sensed distance, or both. The first challenge affects MCL, in that it has to rely more on its odometry, which is prone to error accumulation, and less on precise range measurements, and scan-matching, as there are less measured scan-points, therefore greater insufficiency of information in pairing the virtual scan taken across the map to the reference real laser surface. The second challenge affects MCL, in that the pose estimate is disturbed by noise, and scan-matching, in that noise raises the probability of false correspondences and, in general, erroneous alignment altogether. To this end, we configured the virtual range sensor to operate at a maximum range of 10.0 meters.

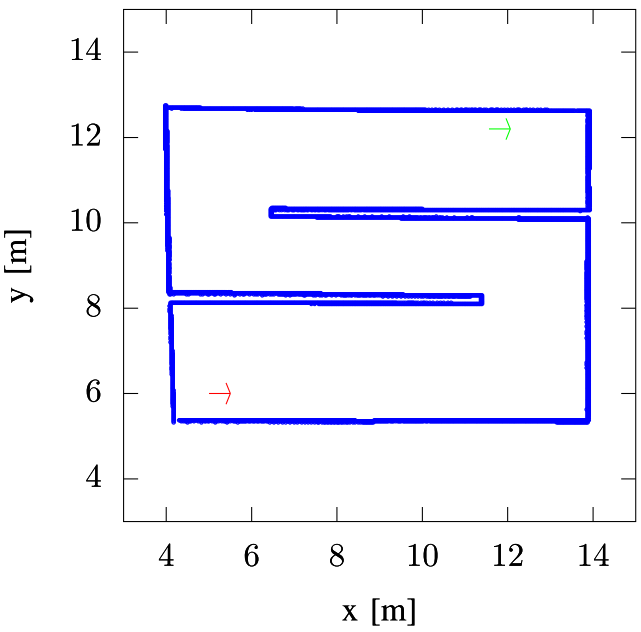

Fig. 4 The map of environment CORRIDOR, M_C. The initial configuration of the robot is seen in green colour, while its goal one in red. The size of the environment is $10 \times 7m^2$

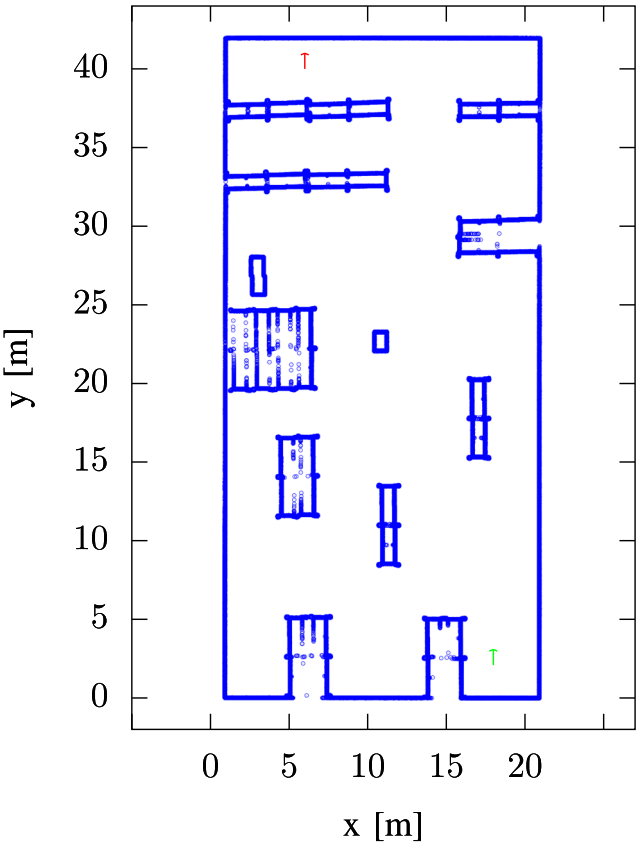

Fig. 5 The map of environment WAREHOUSE, M_W. The initial configuration of the robot is seen in green colour, while its goal one in red. The size of the environment is $20 \times 42m^2$

In all simulations MCL was used along-side KLD sampling, with a minimum number of particles $N_{\min} = 200$ and with a maximum number of particles $N_{\max} = 500$ in both simulated environments.

The initial and goal poses for each map were (a) for M_C: $p_C^i \equiv (11.56\text{m}, 12.20\text{m}, 0.0 \text{ rad})$, and $p_C^g \equiv (5.0\text{m}, 6.0\text{m}, 0.0 \text{ rad})$, respectively, and (b) for M_W: $p_W^i \equiv (17.98\text{m}, 2.08\text{m}, \pi/2 \text{ rad})$ and $p_W^i \equiv (6.0\text{m}, 40.0\text{m}, \pi/2 \text{ rad})$ respectively. The initial and goal poses for each map are drawn in green and red colours in their respective figures.

The robot used is a simulated Turtlebot v.2, equipped with a range sensor of range $r_{max} = 10.0\text{m}$, angular range $\alpha = 260°$ and number of rays $n_r = 640$, whose measurements are corrupted by zero-mean white noise of standard deviation $\sigma = 0.01\text{m}$.

In order to test for the first hypothesis, we conducted simulations with MCL kept in open-loop mode. Denoting by $|\boldsymbol{P}_t|$ the size of the population at time $t > 0$, we conducted $N = 100$ simulations for each particle selection method, comprised of selecting (a) $100\% \times |\boldsymbol{P}_t|$, (b) particles $\{i\}$ from $\boldsymbol{P}_t$ whose weight w_t^i is greater than the population's mean weight $\overline{W_t}$ at time $t > 0$, (c) $10\% \times |\boldsymbol{P}_t|$, and (d) only the particle with the largest weight among all those in $\boldsymbol{P}_t$.

In order to test for the third hypothesis we conducted simulations selecting all $|\boldsymbol{P}_t|$ particles for calculating MCL's final pose, testing the performance of the compound system (Figs. 2 and 3) when the feedback mode used is (a) none (open-loop), (b) soft-1-closed loop, (c) soft-50-closed loop, and (d) hard-closed-loop, as defined in Section 6.

In order to test for the second hypothesis, we observe the results of all $2 \times 4 \times 100$ simulations run in open-loop per particle selection method.

The criterion on which the evaluation of all tests rests is the 2-norm of the total pose error:

$$\|e\|_2 = \left((\hat{x} - x)^2 + (\hat{y} - y)^2 + (\hat{\theta} - \theta)^2\right)^{1/2} \tag{2}$$

where $(\hat{x}, \hat{y}, \hat{\theta})$ is the estimated pose of the robot (estimated by MCL or the system after scan-matching, depending on the context) and (x, y, θ) is its true pose, and was chosen as such because of its expression of the error of the system's state and its ability to provide a centralised locus that facilitates the direct comparison of the performance of each variant of the system in terms of pose accuracy. For every pose output by MCL (denoted by $\hat{\boldsymbol{x}}_t$ in Fig. 2) and the scan-matcher (denoted by $\hat{\boldsymbol{x}}'_t$ in Fig. 2) in one simulation, we record its offset from the actual pose in the form of the 2-norm total error, average it across one simulation and report the distribution of these values across all $N = 100$ simulations of the same configuration. The unit of measurement of the total pose error (2) is $\sqrt{\text{m}^2 + \text{rad}^2}$, and it is omitted in the figures of the following subsections for reasons of economy of space.

Contrary as to the locations where [13] and [15] evaluated their systems' performance (both evaluated their systems' error only in the vicinity of predefined locations), we evaluate it *along the whole path* from p^i to p^g; this offers for a more complete view of the configurations in question.

Simulations were conducted in the Gazebo environment[1] through ROS[2] in Ubuntu 16.04, with a processor of 12 threads, running at 4.00 GHz, using up to 32Gb of RAM. For implementing MCL with KLD sampling we used ROS's `amcl` package[3], which

[1] http://gazebosim.org/

[2] https://www.ros.org/

[3] http://wiki.ros.org/amcl

we modified in order to accommodate particle selection from and particle introduction to the filter's population. The entire system occupies two CPU processes, approximately 300MB of memory, while the scan-matching process utilises approximately 5.2% of one CPU core.

7.1 Results of Tests Regarding Particle Selection Methods

Figures 6 and 7 depict the distributions of the mean 2-norm pose errors of open-loop MCL and of the compound system in environments CORRIDOR and WAREHOUSE per particle selection method respectively. Additional figures that focus on the disdiscernible differences between results of the same distributions are provided in Appendix A.

7.2 Results of Tests Regarding Feedback Methods

Figures 8 and 9 depict the distributions of the mean 2-norm pose errors of MCL and of the compound system in environments CORRIDOR and WAREHOUSE per feedback method respectively. Additional figures that focus on the disdiscernible differences between results of the same distributions are provided in Appendix B.

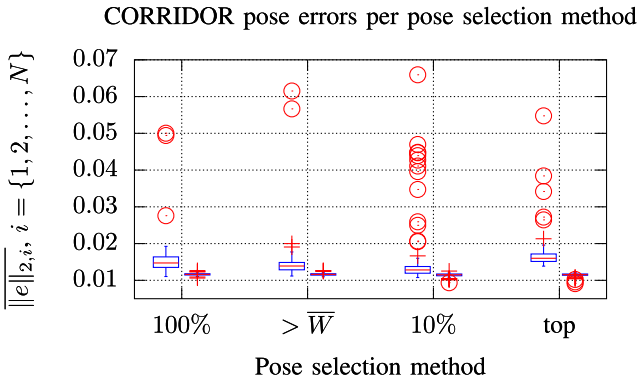

Fig. 6 The distribution of the mean 2-norm total pose error of open-loop-MCL (to the left of each indicated selection method) and of the compound system's (to the right of each indicated selection method) across $N = 100$ simulations according to population selection method in environment CORRIDOR. Signifier "100%" denotes the configuration where all particles of the population set were chosen in the process of weight-averaging for extracting the system's pose estimate, "$> \overline{W}$" that where only those particles whose weight was greater than the particle population's mean weight were selected, "10%" that where only the top 10% of heaviest particles were selected, and "top" the configuration where only the particle with the highest weight among all those in the population was selected as the system's estimate

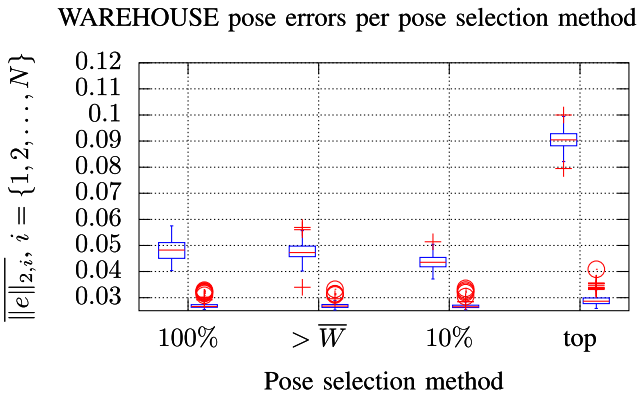

Fig. 7 The distribution of the mean 2-norm total pose error of open-loop-MCL (to the left of each indicated selection method) and of the compound system's (to the right of each indicated selection method) across $N = 100$ simulations according to population selection method in environment WAREHOUSE. Signifier "100%" denotes the configuration where all particles of the population set were chosen in the process of weight-averaging for extracting the system's pose estimate, "$> \overline{W}$" that where only those particles whose weight was greater than the particle population's mean weight were selected, "10%" that where only the top 10% of heaviest particles were selected, and "top" the configuration where only the particle with the highest weight among all those in the population was selected as the system's estimate

8 Discussion

8.1 Particle Selection Methods

As regards particle selection, we focus on the errors of open-loop MCL, where the performance of each particle selection

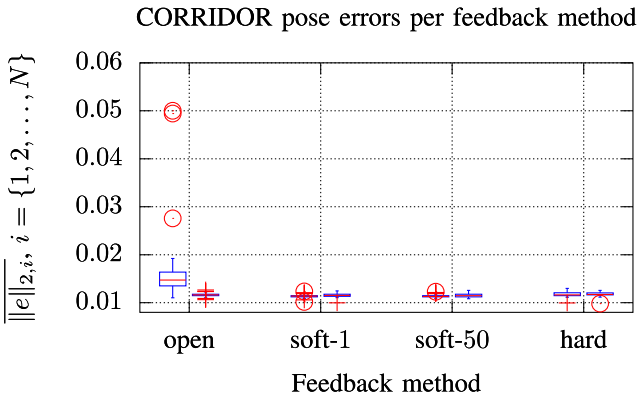

Fig. 8 The distribution of the mean 2-norm total pose error of MCL (to the left of each indicated feedback method) and of the compound system's (to the right of each indicated feedback method) across $N = 100$ simulations according to feedback method in environment CORRIDOR. Signifier "open" is shorthand for open-loop, meaning that no particle of the overall system is fed back to the particle filter, "soft-1" for the configuration where the overall system's output is fed back to the particle filter in the form of one particle, "soft-50" for that where it is fed back in the form of as many particles as half of the population's size, and "hard" for the configuration where the particle filter is initialised around the pose calculated after scan-matching

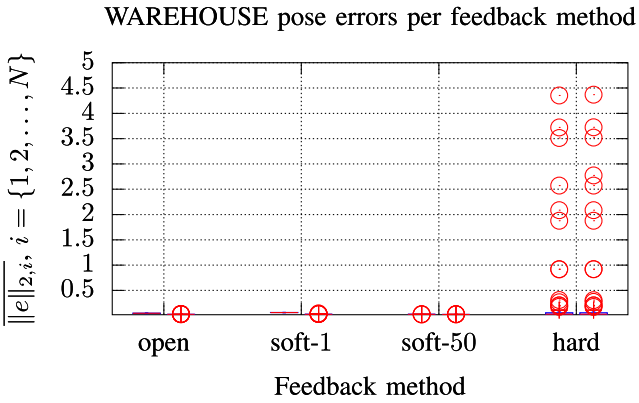

Fig. 9 The distribution of the mean 2-norm total pose error of MCL (to the left of each indicated feedback method) and of the compound system's (to the right of each indicated feedback method) across $N = 100$ simulations according to feedback method in environment WAREHOUSE. Signifier "open" is shorthand for open-loop, meaning that no particle of the overall system is fed back to the particle filter, "soft-1" for the configuration where the overall system's output is fed back to the particle filter in the form of one particle, "soft-50" for that where it is fed back in the form of as many particles as half of the population's size, and "hard" for the configuration where the particle filter is initialised around the pose calculated after scan-matching

method can be discerned with clarity as it is unadulterated by feedback or the performance of scan-matching. Turning our attention to Figs. 6 and 7 (more closely: Figs. 11 and 12), we first of all discern that selecting particles whose weight is larger than that of the mean population weight at the time of their selection results in lower pose errors compared to selecting all particles, in both simulated environments, but only slightly. This effect is intuitively reasonable since one expects that particles which contribute to the overall pose with a weight lower than the mean population weight have overall negative contribution to the pose accuracy, which, as it now seems, is near-negligible. Furthermore, in contrast to the other two selection practices introduced, this one is less destructive since it anchors its discarding practice on the varying mean population weight, and therefore selects particles whose number is dynamic, rather than anchoring it on the number of heavy-most particles and selecting particles whose number is static.

That said, selecting the top 10% percent of particles at each iteration outperforms selecting particles whose weight is larger than the mean population weight; the improvements in both environments is measured in millimeters, but the pattern is the same: selecting the top 10% percent of all particles at each iteration outperforms selecting particles whose weight is larger than the population's mean weight at the time of their selection, which, in turn, outperforms vanilla MCL.

What is counter-intuitive is the increased pose errors in both environments when only the single heaviest particle is selected as the filter's pose estimate: what one would expect is that the particle of the highest weight, that is the particle whose pose estimate explains the incoming measurements best within its population and which is then, in theory, the filter's best estimate, would exhibit the lowest pose error, but, in actuality, it is less accurate than the collective estimate of the filter. This discrepancy indicates that there is a threshold level at which the tested hypothesis is confirmed and that, given the evidence, the particle that accounts for incoming measurements the best does not hold the best credibility compared to that of the population as a collective. This essentially is the theory behind not rejecting low-weighted particles, since the best particle can be optimal locally (for the last iterations) but not globally. This behaviour prompts us to consider that a particle filter may not be viewed as an aggregation of separate estimates but as a collection of estimate-fragments, where no one can substitute for the whole without irretrievable loss of information and estimation quality decrease. This reversal in estimation quality may be attributed to the marginalisation of all information that the rest of the population carries, including the randomness that KLD sampling introduces as it generates new particles.

This behaviour does not cast a shadow on the method of selecting the top 10% of heavy-most particles, as, although it points to the possibility that it would enjoy the same fate had the minimum population size been significantly lower, the credibility of the filter would be at stake too with such a low minimum population size; at any rate, a low minimum population size is disadvised with regard to both the overall population's quality of estimate (particle depletion is the danger here) and that of a subset of it.

8.2 As Regards the Decrease of the Pose Error Due to Scan-Matching

In general, the pose output by scan-matching is less erroneous than that output by MCL across all configurations of different selection methods in open-loop mode (Figs. 6 and 7), with the error decrease ranging from a few millimeters (in the case of the simple map CORRIDOR) to a few centimeters (in the case of the more complex map WAREHOUSE).

8.3 Feedback Methods

As regards feedback regimes, the difference in performance between the soft-50 loop closure method and vanilla MCL with regard to the MCL output pose is distinguishable: the former's pose errors are approximately 43% lower than those of the latter in open-loop in environment WAREHOUSE, and approximately 25% lower in environment CORRIDOR. However, that between the former and the latter with regard to the output of scan-matching is very slight

in both cases, with the pose errors of soft-50 being slightly less erroneous than the open-loop ones.

The difference in performance of soft-50 loop closure compared to that of soft-1 loop closure is negligible in the simple environment CORRIDOR, with the former achieving slightly better pose errors, regarding both the output of MCL and that of MCL followed by scan-matching. However, in the complex map of WAREHOUSE, the difference in performance in favor of the former is distinguishable, especially when examining the pose errors of MCL, where the former's errors are decreased by almost 60%. The difference in performance between the two with regard to the errors of the poses output by scan-matching is again slight (measured in millimeters).

When comparing the difference in performance between the soft-50 loop closure method and the hard loop closure method, we observe that, in terms of median values, they are close, with the former outperforming the latter overall. What is striking though is the difference in their performance in environment WAREHOUSE: under the hard loop closure regime, the system was unable to recover from severe pose errors, as the filter's population was initialised anew on every pose output by scan-matching, regardless of its accuracy. Conversely, assuming that, statistically, a number of errors arose too in the simulations where the soft-50 loop closure was employed, this behaviour was absent. The reason for this robust behaviour is that, in soft-p loop closure mode, when an erroneous pose is output by scan-matching, this pose is incorporated into the filter in the form of particles whose total number is lower than the population size. After their introduction to the population, the filter internally assigns a weight to each one (Section 4), and, as these particles' poses are severely erroneous, this is reflected on the values of their weights, as these poses account for the incoming measurements rather poorly. Since MCL's output pose is the weighted average of all the population's estimates, these particles participate in the final voting at a minuscule rate, and, therefore, the filter's estimate is largely undisturbed by them, exhibiting the same robust behaviour as vanilla MCL, but with improved pose estimates. The advantage of incorporating KLD sampling to MCL is that these particles, whose weight is minuscule, are then rejected from the particle population, leaving them no space to influence its internal estimate cohesion in the subsequent iterations.

8.4 Conclusions on Combinatory Configurations

With the exception of the sub-hypothesis that selecting the heaviest particle off MCL would yield improved results over vanilla MCL, the three hypotheses stated in Section 7 were proven to be true given the evidence presented in Sections 7.1 and 7.2. However, caution must be advised in to that combining any two true hypotheses would not necessarily prove to be also true. Consider for instance hypotheses H2 and H3, and let us formulate their combined hypothesis, H4, that states that under the soft-50 loop closure regime the output of the overall system is more accurate than the output of MCL. A close look in Fig. 13 shows that H4 is clearly false[4]. Likewise, it would be precarious to assume that, for instance, the same conclusions would be drawn for hypothesis H1 if any form of feedback substituted the open-loop mode, or, in general, a combination of any hypothesis or sub-hypothesis with any other would yield the same conclusion.

9 Conclusions and Future Steps

This paper introduced a localisation system that consists of a particle filter combined with population selection, tandem scan-matching, and feedback, as a means of improving the localisation estimate of vanilla particle filters (MCL).

To the best of our knowledge, the contribution to the field is novel, and consists of two separate components. The first concerns the inference of a particle filter's estimated pose, and argues that, in view of the proportionality of a particle's weight and its estimation accuracy, discarding low-weight particles from the filter's population yields increased pose accuracy. Our motivation for research into the topic of pose selection arises from the apparent insufficiency of prosthetic measures used to enhance the accuracy of a particle filter. The second concerns the manner of feeding back the result of scan-matching the scan captured from the robot's physical range scan sensor and a scan captured from the filter's estimated pose, derived by means of ray-casting within the map. Our motivation for research into the topic of pose feedback in tandem combinations of particle filters with scan-matching arises from the shortcomings

[4]The reason for this effect is the following: as aforementioned, the pose output by the scan-matching block in Fig. 2 is the result of applying the relative roto-translation between a scan captured from the robot's physical range-finder sensor located at its actual pose and a scan captured from MCL's estimated pose within the map via the means of ray-casting to MCL's estimated pose. Since the map is a grid of finite resolution, ray-casting can only discern differences in range of up to one grid size − in our case $\texttt{grid\_size} = 0.01\text{m}$ −, which means that, if the map represented the physical environment perfectly and, because the range is computed from the center of the grid, the maximum range error per ray would be $\texttt{grid\_size}/\sqrt{2} = 0.0071\text{m}$. However, since (a) the map is not given in the form of an architect's exact floor plan but is constructed via probabilistic means (in this case ROS's `open_karto` package), (b) computing the range from a grid cell's center introduces orientation errors per ray, (c) the rays of the scan from the physical range-finder sensor are subject to disturbance, and (d) the scan-matching method employed is not perfect, the error introduced inevitably rises, and the performance of the scan-matching block is therefore inevitably limited to further than if the above sources of error were absent.

Fig. 10 Program logo

European Union
European Regional Development Fund
EPAnEK 2014–2020
OPERATIONAL PROGRAMME
COMPETITIVENESS ENTREPRENEURSHIP INNOVATION
Co-financed by the European Union and Greek national funds
ΕΣΠΑ 2014-2020
ανάπτυξη - εργασία - αλληλεγγύη
Partnership Agreement 2014-2020

of the two methods found currently in the literature. The merits of the newly introduced feedback regime address these shortcomings, and consist of increased robustness in comparison to one feedback manner found in the literature, and increased pose accuracy in comparison to the second feedback manner of the relevant literature.

More specifically, we formulated hypotheses that (a) discarding low-weight particles from the filter's calculation of its final pose estimate increases its pose accuracy (in open-loop), (b) applying the roto-translation obtained through scan-matching a scan captured from the robot's real pose and a scan captured via ray-casting the map of the robot's environment from MCL's estimated pose to it yields decreased pose errors, and (c) introducing the improved pose to MCL's population in the form of a multitude of particles results in increased pose accuracy compared to open-loop MCL, increased robustness compared to initialising MCL anew with this estimate [13], and increased pose accuracy compared to introducing it in the form of only one particle [14].

We tested these hypotheses in two disparate environments in simulation and found that, given the evidence, all were true except for that which states that picking the heaviest particle off of MCL as its estimate results in increased pose accuracy compared to picking all particles and weight-averaging their poses. This latter result could be especially informative to the pose selection methods found today in the literature [11, 12], which use the highest-weighted particle as the filter's pose estimate in fail-safe circumstances.

The resulting augmented system described herein admits configurations which are a superset of configurations of state-of-the-art systems.

This study will, in the future, be extended to investigate means of selecting particles from MCL's population other than strictly elementary weight-based ones. For instance, particles of the highest-weighted mode could be first clustered by weight, or spatial spread, or both, and then selected by being conditioned on some static or varying threshold that is a function of that mode's statistic characteristics Fig. 10.

Acknowledgments This research has been co-financed by the European Union and Greek national funds through the Operational Program Competitiveness, Entrepreneurship and Innovation, under the call RESEARCH CREATE INNOVATE (project code:T1EDK-03032).

Appendix A

This section features magnified versions of the figures found in Sections 7.1 and 7.2 for the use of drawing clearer comparisons between results of different selection (Section A) and feedback (Section B) methods.

A Focused Results of Tests on Selection Methods

Figures 11 and 12 comprise the distributions of the mean 2-norm total pose error of open-loop MCL per selection method tested across $N = 100$ simulations, as seen in Figs. 6 and 7 respectively, focused here for clarity of comparison purposes.

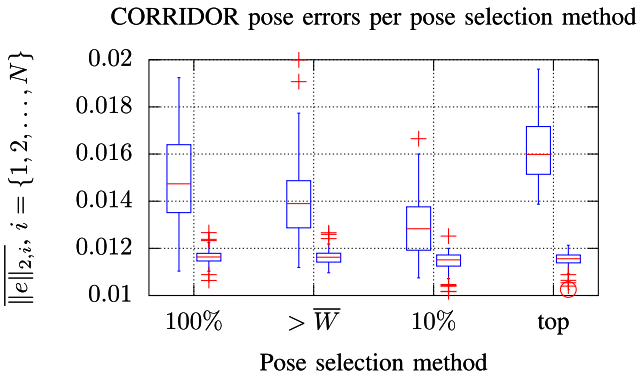

Fig. 11 The distribution of the mean 2-norm total pose error of open-loop-MCL (to the left of each indicated selection method) and of the compound system's (to the right of each indicated selection method) across $N = 100$ simulations according to population selection method in environment CORRIDOR, focused for clarity of comparison

B Focused Results of Tests on Feedback Methods

Figures 13 and 14 comprise the distributions of the mean 2-norm total pose error of open-loop MCL per feedback method tested across $N = 100$ simulations, as seen in Figs. 8 and 9 respectively, focused here for clarity of comparison purposes.

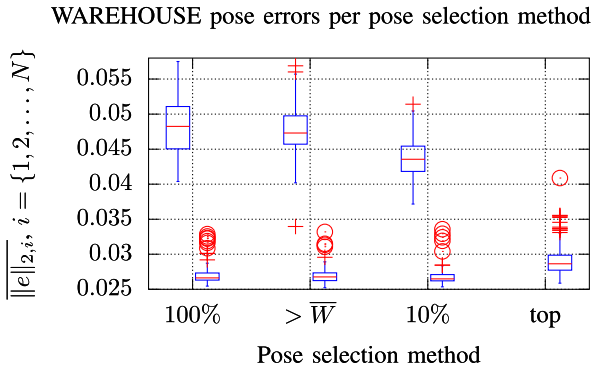

Fig. 12 The distribution of the mean 2-norm total pose error of open-loop-MCL (to the left of each indicated selection method) and of the compound system's (to the right of each indicated selection method) across $N = 100$ simulations according to population selection method in environment WAREHOUSE, focused for clarity of comparison

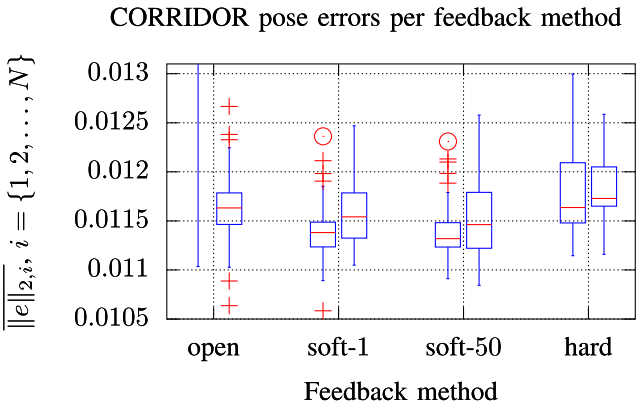

Fig. 13 The distribution of the mean 2-norm total pose error of MCL (to the left of each indicated feedback method) and of the compound system's (to the right of each indicated feedback method) across $N = 100$ simulations according to feedback method in environment CORRIDOR, focused for clarity of comparison

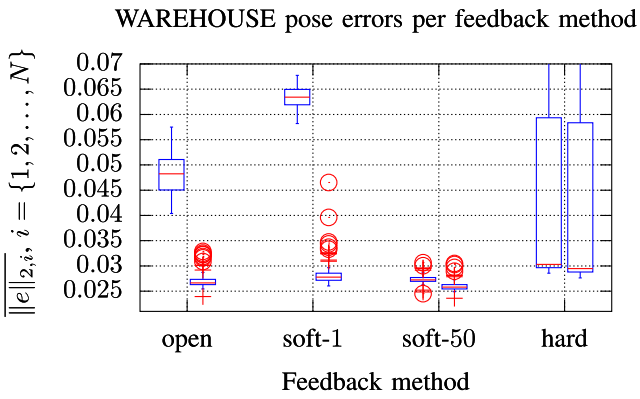

Fig. 14 The distribution of the mean 2-norm total pose error of MCL (to the left of each indicated feedback method) and of the compound system's (to the right of each indicated feedback method) across $N = 100$ simulations according to feedback method in environment WAREHOUSE, focused for clarity of comparison

References

1. Thrun, S., Burgard, W., Fox, D.: Probabilistic robotics (intelligent robotics and autonomous agents). MIT Press, Cambridge (2005)
2. Dellaert, F., Fox, D., Burgard, W., Thrun, S.: Monte Carlo localization for mobile robots. In: Proceedings 1999 IEEE international conference on robotics and automation (Cat. No.99CH36288C), Detroit, MI, USA, vol. 2, pp. 1322–1328 (1999). https://doi.org/10.1109/ROBOT.1999.772544
3. Maybeck, P.: Stochastic Models, Estimation and Control, vol. 1. Academic Press, New York (1979)
4. Gutmann, J., Konolige, K.: Incremental mapping of large cyclic environments. In: Proceedings 1999 IEEE international symposium on computational intelligence in robotics and automation. CIRA'99 (Cat. No.99EX375), Monterey, CA, USA, pp. 318–325 (1999). https://doi.org/10.1109/CIRA.1999.810068
5. Hahnel, D., Burgard, W., Fox, D., Thrun, S.: An efficient fastSLAM algorithm for generating maps of large-scale cyclic environments from raw laser range measurements. In: Proceedings 2003 IEEE/RSJ international conference on intelligent robots and systems (IROS 2003) (Cat. No.03CH37453), Las Vegas, NV, USA, vol. 1, pp. 206–211 (2003). https://doi.org/10.1109/IROS.2003.1250629
6. Wang, C.-C., Thorpe, C., Thrun, S.: Online simultaneous localization and mapping with detection and tracking of moving objects: theory and results from a ground vehicle in crowded urban areas. In: 2003 IEEE international conference on robotics and automation (Cat. no.03CH37422), Taipei, Taiwan, vol. 1, pp. 842–849 (2003). https://doi.org/10.1109/ROBOT.2003.1241698
7. Lacroix, S., Mallet, A., Bonnafous, D., Bauzil, G., Fleury, S., Herrb, M., Chatila, R.: Autonomous rover navigation on unknown terrains: functions and integration. Int. J. Robot. Res. **21**(10–11), 917–942 (2002). https://doi.org/10.1177/027836490202101084
8. Minguez, J., Montesano, L., Anc Montano, L.: An architecture for sensor-based navigation in realistic dynamic and troublesome scenarios. In: 2004 IEEE/RSJ international conference on intelligent robots and systems (IROS) (IEEE Cat. No.04CH37566), 3, vol. 3, pp. 2750–2756 (2004)
9. Montesano, L., Minguez, J., Montano, L.: Modeling dynamic scenarios for local sensor-based motion planning. Auton. Robot. **25**, 231–251 (2008)
10. Schulz, D., Burgard, W., Fox, D., Cremers, A.B.: Tracking multiple moving targets with a mobile robot using particle filters and statistical data association. In: Proceedings 2001 ICRA. IEEE international conference on robotics and automation (Cat. No.01CH37164), Seoul, South Korea, vol. 2, pp. 1665–1670 (2001). https://doi.org/10.1109/ROBOT.2001.932850
11. Coltin, B.rian., Manuela, M.V.: Multi-Observation sensor resetting localization with ambiguous landmarks. Autonomous robots 35. https://doi.org/10.1007/s10514-013-9347-y (2011)
12. Liemhetcharat, S., Coltin, B., Veloso, M.M.: Vision-based cognition of a humanoid robot in standard platform robot soccer (2010)
13. Vasiljevic, G., Miklic, D., Draganjac, I., Kovacic, Z., Lista, P.: High-accuracy vehicle localization for autonomous warehousing (2016)
14. Peng, G., Zheng, W., Lu, Z., et al.: An improved AMCL algorithm based on laser scanning match in a complex and unstructured environment. Complexity **2018**, 11 (2018). Article ID 2327637, https://doi.org/10.1155/2018/2327637
15. Röwekämper, J., Sprunk, C., Tipaldi, G.D., Stachniss, C., Pfaff, P., Burgard, W.: On the position accuracy of mobile robot localization based on particle filters combined with

scan matching. In: 2012 IEEE/RSJ international conference on intelligent robots and systems, Vilamoura, pp. 3158–3164 (2012). https://doi.org/10.1109/IROS.2012.6385988
16. Fox, D.: Adapting the sample size in particle filters through KLD-sampling. Int J Robot Res **22**(12), 985–1003 (2003). https://doi.org/10.1177/0278364903022012001
17. Censi, A.: An ICP variant using a point-to-line metric. In: 2008 IEEE international conference on robotics and automation, Pasadena, CA, pp. 19–25 (2008). https://doi.org/10.1109/ROBOT.2008.4543181
18. Besl, P.J., McKay, N.D.: A method for registration of 3-D shapes. IEEE Transactions on Pattern Analysis and Machine Intelligence **14**(2), 239–256 (1992). https://doi.org/10.1109/34.121791, ISSN 0162-8828
19. Grimson, W., Eric L.: Object recognition by computer: the role of geometric constraints. MIT Press, Cambridge (1990). ISBN 0-262-07130-4
20. Lu, F., Milios, E.: Robot pose estimation in unknown environments by matching 2D range scans. J Intell Robot Syst **18**(3), 249–275 (1997). https://doi.org/10.1023/A:1007957421070, ISSN 1573-0409
21. Pfister, S.T., Kriechbaum, K.L., Roumeliotis, S.I., Burdick, J.W.: Weighted range sensor matching algorithms for mobile robot displacement estimation. In: Proceedings 2002 IEEE international conference on robotics and automation (Cat. No.02CH37292), Washington, DC, USA, vol. 2, pp. 1667–1674 (2002). https://doi.org/10.1109/ROBOT.2002.1014782
22. Chetverikov, D., Svirko, D., Stepanov, D., Krsek, P.: The trimmed iterative closest point algorithm. In: Object recognition supported by user interaction for service robots, Quebec City, Quebec, Canada, vol. 3, pp. 545–548 (2002). https://doi.org/10.1109/ICPR.2002.1047997
23. Rousseeuw, P.J.: Least median of squares regression. J Ame Stat Assoc **79**, 871–880 (1984). Taylor & Francis, https://doi.org/10.1080/01621459.1984.10477105
24. Biber, P., Strasser, W.: The normal distributions transform: a new approach to laser scan matching. In: Proceedings 2003 IEEE/RSJ international conference on intelligent robots and systems (IROS 2003) (Cat. No.03CH37453), Las Vegas, NV, USA, vol. 3, pp. 2743–2748 (2003). https://doi.org/10.1109/IROS.2003.1249285
25. Atkinson, K.: An introduction to numerical analysis, 2nd edn, ISBN: 978-0-471-62489-9 (1989)
26. Zezhong, X., Jilin, L., Zhiyu, X.: Scan matching based on CLS relationships. In: IEEE international conference on robotics, intelligent systems and signal processing, 2003. Proceedings. 2003, Changsha, Hunan, China, vol. 1, pp. 99–104 (2003). https://doi.org/10.1109/RISSP.2003.1285556
27. Censi, A., Iocchi, L., Grisetti, G.: Scan matching in the hough domain. In: Proceedings of the 2005 IEEE international conference on robotics and automation, pp. 2739–2744 (2005)
28. Montesano, L., Minguez, J., Montano, L.: Probabilistic scan matching for motion estimation in unstructured environments. In: 2005 IEEE/RSJ international conference on intelligent robots and systems, Edmonton, Alta, pp. 3499–3504 (2005). https://doi.org/10.1109/IROS.2005.1545182
29. Diosi, A., Kleeman, L.: Laser scan matching in polar coordinates with application to SLAM. In: 2005 IEEE/RSJ international conference on intelligent robots and systems, Edmonton, Alta, pp. 3317–3322 (2005). https://doi.org/10.1109/IROS.2005.1545181
30. Minguez, J., Lamiraux, F., Montesano, L.: Metric-Based Scan matching algorithms for mobile robot displacement estimation. In: Proceedings of the 2005 IEEE international conference on robotics and automation, Barcelona, Spain, pp. 3557–3563 (2005). https://doi.org/10.1109/ROBOT.2005.1570661
31. Olson, E.B.: Real-time correlative scan matching. In: 2009 IEEE international conference on robotics and automation, Kobe, pp. 4387–4393 (2009). https://doi.org/10.1109/ROBOT.2009.5152375
32. Chen, F., Inderjit, C., Omri, R.: Perimeter-based polar scan matching (PB-PSM) for 2D laser Odometry. J Intell Robot Syst **80**, 231–254 (2015). ISSN 1573-0409, https://doi.org/10.1007/s10846-014-0158-y
33. Konecny, J., Prauzek, M., Kromer, P., Musilek, P.: Novel point-to-point scan matching algorithm based on cross-correlation, Mobile Information Systems (2016)
34. Sandberg, D., Wolff, K., Wahde, M.: A robot localization method based on laser scan matching, Advances in Robotics, pp. 171–178. Springer, Berlin (2009). isbn 978-3-642-03983-6
35. Zhu, J., Zheng, N., Yuan, Z.: An Improved technique for robot global localization in indoor environments. International Journal of Advanced Robotic Systems. https://doi.org/10.5772/10525 (2011)
36. Beinschob, P., Reinke, C.: Advances in 3D data acquisition, mapping and localization in modern large-scale warehouses. In: 2014 IEEE 10th international conference on intelligent computer communication and processing (ICCP), Cluj Napoca, pp. 265–271 (2014). https://doi.org/10.1109/ICCP.2014.6937007
37. Cummins, M., Newman, P.: Probabilistic appearance based navigation and loop closing. In: Proceedings 2007 IEEE international conference on robotics and automation, Roma, pp. 2042–2048 (2007). https://doi.org/10.1109/ROBOT.2007.363622
38. Cherubini, A.ndrea., Colafrancesco, M., Oriolo, G., Freda, L., Chaumette, F.: Comparing appearance-based controllers for Nonholonomic navigation from a visual memory. In: ICRA 2009 workshop on safe navigation in open and dynamic environments: application to autonomous vehicles, Kobe, Japan, Japan (2009)
39. Sprunk, C., Tipaldi, G.D., Cherubini, A., Burgard, W.: Lidar-based teach-and-repeat of mobile robot trajectories. In: 2013 IEEE/RSJ international conference on intelligent robots and systems, Tokyo, pp. 3144–3149 (2013). https://doi.org/10.1109/IROS.2013.6696803
40. Smith, A.F.M., Gelfand, A.E.: Bayesian statistics without tears: a Sampling–Resampling perspective. Ame. Stat. **46**(2), 84–88 (1992). https://doi.org/10.1080/00031305.1992.10475856
41. Zhu, Q., başar, T.: Robust and resilient control design for cyber-physical systems with an application to power systems. In: Proceedings of the IEEE conference on decision and control, pp. 4066–4071 (2011). https://doi.org/10.1109/CDC.6161031
42. Tavana, M., Busch, T.E., Davis, E.L.: Fuzzy multiple criteria workflow robustness and resiliency modeling with petri Nets. IJKBO, 1, 72–90 (2011)
43. Tzitzis, A., Megalou, S., Siachalou, S., Yioultsis, T., Kehagias, A., Tsardoulias, E., Filotheou, A., Symeonidis, A., Petrou, L., Dimitriou, A.G.: Phase ReLock - localization of RFID tags by a moving robot, to appear in the european conference on antennas and propagation, Krakow, Poland (2019)
44. Megalou, S., Tzitzis, A., Siachalou, S., Yioultsis, T., Sahalos, J., Tsardoulias, E., Filotheou, A., Symeonidis, A., Petrou, L., Bletsas, A., Dimitriou, A.G.: Fingerprinting localization of RFID tags with real-time performance-assessment, using a moving robot, to Appear in the european conference on antennas and propagation, Krakow, Poland (2019)

Alexandros Filotheou received his diploma in Electrical and Computer Engineering from the Aristotle University of Thessaloniki (AUTh), Greece, in 2013 and his MSc in Systems, Control, and Robotics from the Royal Institute of Technology (KTH), Stockholm, Sweden, in 2017. He is currently a PhD candidate at AUTh. His research interests focus on control and localisation of robotic systems.

Emmanouil Tsardoulias Emmanouil has obtained his doctorate and engineering diploma from the Department of Electrical and Computer Engineering at Aristotle University of Thessaloniki (AUTH), Greece, in 2013 and 2007 respectively. His working experience includes participation in the ?Eudoxus? project with the collaboration of Ministry of Education and the EU project RAPP (FP7-ICT-610947) among others. His research interests are focused in Robotics and specifically in Autonomous Robots (ground or aerial). Some of the topics involved are autonomous navigation, SLAM (Simultaneous Localization and Mapping), multi-robot exploration / full coverage, robotic architectures oriented for the creation of robotic applications and robot-agnostic RESTful APIs. In addition, from 2009 till now, is the technical manager of the artificial intelligence group of the P.A.N.D.O.R.A. and R4A robotics teams, which operate at the School of Electrical and Computer Engineering, Aristotle University of Thessaloniki. PANDORA has participated in five world-wide RoboCup competitions, achieving the second place in the Autonomy finals twice.

Antonis Dimitriou received the diploma and the Ph.D degree in Electrical and Computer Engineering from the Aristotle University of Thessaloniki, Greece, in 2001, and 2006 respectively. Since 2007, he is with the School of Electrical and Computer Engineering of AUTh, where he currently serves as a teaching and research faculty member. He has participated in more than 20 research projects, 8 of which since 2007 as a principal investigator in the fields of Robotics, RFIDs, and Wireless Sensor Networks. He is currently the coordinator of projects "CultureID" and "RELIEF"; both involve prototype SLAM-capable terrestrial robots and drones, equipped with UHF RFID technology. He was a Management Committee Member in the ICT COST Action IC301 "Wireless Power Transmission for Sustainable Electronics (WiPE)". He is the author or co-author of approximately 60 journal or conference papers and a book-chapter. Dr. Dimitriou was the recipient of the Ericsson Award of Excellence in Telecommunications in 2001 and co-recipient of the student-paper award in the 2011 IEEE RFID-TA conference. He received the "IEEE Wireless Communications Letters Exemplary Reviewer" award in 2012 and 2014. He is a Senior IEEE Member since February 2014. He also serves as a reviewer for major journals and as a TPC member for international conferences.

Andreas Symeonidis Symeonidis is an Associate Professor with the Department of Electrical and Computer Engineering at the Aristotle University of Thessaloniki, Greece and the Chief Research Officer at Cyclopt.com. His research interests include Software engineering processes, Model-driven engineering, Software quality and Software analytics, Middleware Robotics and Knowledge extraction from big data repositories. Dr. Symeonidis? work has been published in over 130 papers, book chapters, and conference publications. He is co-author of the books ?Agent Intelligence through Data Mining? (Springer publishing), ?Mining Software Engineering Data for Software Reuse? (Springer publishing) and ?Practical Machine Learning in R? (Leanpub publishing). He is currently coordinating more than 10 contract R&D projects, while serving occasionally as a R&D project evaluator and reviewer for the European Commission. More at: http://users.auth.gr/symeonid

Loukas Petrou Associate Professor at the Department of Electrical and Computer Engineering, Aristotle University of Thessaloniki Greece, received the Diploma in Electrical Eng., from the University of Patras Greece, the M. Sc. in Theory and Practice of Automatic Control from U.M.I.S.T., Manchester U.K. and the Ph.D. in Elec. Eng., from Imperial College, London U.K. His research interests include microprocessor applications, autonomous mobile robots, intelligent control of waste water treatment plants, reconfigurable embedded systems, evolutionary computation, fuzzy logic and neural network control systems.